Rotary resonance recoupling for half-integer quadrupolar nuclei in solid-state nuclear magnetic resonance spectroscopy

Sungsool Wi, John W. Logan, Dimitris Sakellariou, Jamie D. Walls, and Alexander Pines[a)]
Materials Sciences Division, Lawrence Berkeley National Laboratory and Department of Chemistry, University of California at Berkeley, Berkeley, California 94720

(Received 7 June 2002; accepted 24 July 2002)

Investigations were made of rotary resonance recouplings (R^3) of chemical shift anisotropy (CSA), heteronuclear dipolar (HTD), and homonuclear dipolar (HMD) couplings involving half-integer quadrupolar nuclei under magic-angle sample spinning condition. Under rotary resonance conditions provided by a low amplitude rf field and a high spinning speed, the spectrum of the central transition coherence of half-integer quadrupolar nuclei shows recouplings of CSA, HTD, and HMD interactions that depend on the ratio of the rf field to the spinning speed. These new properties can be used to extract electronic and structural information about the sample that are otherwise difficult to extract in the presence of a dominant quadrupolar interaction. An average Hamiltonian theory is used to explain the recoupling properties of various interactions. Experimental implementations of the R^3 are demonstrated on model compounds with spin-3/2 systems. © *2002 American Institute of Physics.* [DOI: 10.1063/1.1506907]

I. INTRODUCTION

Magic-angle-spinning (MAS) solid state nuclear magnetic resonance (NMR) provides high resolution spectra of systems containing spin-1/2 nuclei by removing anisotropic interactions, such as the dipolar coupling and chemical shift anisotropy (CSA) that characterize the structure and electronic environments of atoms in molecules.[1,2] Combined with cross polarization[3,4] (CP) and high power proton decoupling,[3,5–8] the MAS method in solid state NMR has been a fascinating topic for the past few decades.

Various recoupling methods, which reintroduce CSA, heteronuclear dipolar (HTD), or homonuclear dipolar (HMD) interactions while retaining site specific resolution provided by MAS, have been widely incorporated for electronic and structural elucidation of systems involving spin-1/2 nuclei.[9–16]

In systems involving quadrupolar nuclei ($S \geqslant 1/2$), spin dynamics are complicated by the extra quadrupolar anisotropy, which is usually the dominating coupling among the various interactions. The spectrum of the central transition $|1/2\rangle \leftrightarrow |-1/2\rangle$ of half-integer quadrupolar nuclei is not affected by the first-order quadrupolar interaction,[17] however it is broadened by the second-order quadrupolar interaction which contains zero-, second-, and fourth-rank spatial tensors. The fourth-rank anisotropic term of the second-order quadrupolar interaction does not vanish under fast MAS.[18–20] Challenges also arise from the fact that the applied rf nutation fields have to compete with much larger internal coupling frequencies stemming from the quadrupole interaction. Most MAS recoupling techniques available for the spin-1/2 system involving radio frequency (rf) irradiation are thus not feasible for quadrupolar spin systems.

Population transfers via rotor-synchronized adiabatic passages applicable for manipulating strongly coupled quadrupolar sites have been developed.[21] Under continuous rf irradiation, quadrupolar I_z states are reshuffled adiabatically when MAS nullifies the first-order quadrupolar effect modulated by the spinning frequency. As for all crystallites, the nullifications occurring per rotor period result in an interference with spatial terms of the dipolar coupling oscillating at $\pm\omega_r$, $\pm 2\omega_r$ and provide a net reintroduction of the dipolar coupling. This principle underlies the continuous transfer of populations by double resonance (TRAPDOR) method[22–24] as well as the recoupling by adiabatic passage double resonance (REAPDOR) technique.[25–27] Adiabatic passage is efficient only in the moderately slow spinning regime and under high rf power and is therefore less applicable when fast spinning and/or low rf field are mandatory.

Homonuclear spin–spin interactions in quadrupolar nuclei were discussed based on six-quantum excitation[28,29] or spin diffusion caused by the flip–flop terms[30] of a spin-3/2 pair in the context of the MQMAS experiment.[31,32] Moreover, Edén *et al.* reported the reintroduction of homonuclear dipolar coupling between quadrupolar nuclei caused by the interference of the first-order quadrupolar interaction with the dipolar interaction under MAS, resulting in a broadening of the MAS line shape.[33] A similar observation in a deuterium sample was also reported earlier by Facey *et al.*[34,35]

A heteronuclear dipolar recoupling scheme involving the overtone mode of ^{14}N($I=1$) irradiated at twice the Larmor frequency also has been reported.[36,37] Here, the MAS modulated nutation frequency of the second-order quadrupolar interaction, the only broadening mechanism for a spin-1 nucleus under overtone irradiation, has a periodicity tied to the rotor spinning frequency. The interference between the

a)Author to whom correspondence should be addressed. Electronic mail: pines@cchem.berkeley.edu

second-order quadrupolar interaction and the dipolar interaction, which is also modulated with the rotor spinning periodicity under MAS, causes a dephasing of the echo-signal encoded in an *S* nucleus (either a spin-1/2 nucleus or the central transition of any half-integer quadrupolar spin) which is directly bonded to ^{14}N.

Recently, a rotary resonance (RR) effect has been incorporated for efficient multiple quantum preparation and conversion into central transition coherence (CTC) in the MQMAS experiment using a low rf field and high spinning speed.[38,39] Two different approaches to the preparation of the multiple quantum coherence (MQC) were suggested; preparation of MQC from the equilibrium *z* magnetization or generation of MQC from the CTC.[38] In the former case, MQC excitation occurs at rf field strengths between adjacent RR conditions, $\omega_{\mathrm{rf}}=2n\omega_r/(S+1/2)$ $(n=1,2,\ldots)$, whereas in the latter case an efficient MQC excitation occurs at RR conditions. In both cases, the spin-locking efficiencies of the CTC and the MQC are poor at the RR conditions because they propagate to other coherences. Conversion of MQC to CTC during the detection step is most efficient at $\omega_{\mathrm{rf}}=n\omega_r(n=1,2,\ldots)$ conditions. A related phenomenon, used for HMD recouplings among half-integer quadrupolar nuclei, was reported by Baldus *et al.*[40] Under a spin-locking condition provided by fast MAS and low rf field strengths, rf-driven 2D-correlational cross peaks between homonuclear quadrupolar nuclei were observed based on the double-quantum mode of coherence transfer among the CTCs of quadrupolar nuclei at $\omega_{\mathrm{rf}}=\omega_r/(2S+1)$.

In this work, the reintroduction of various interactions such as CSA, HTD and HMD terms involving quadrupolar nuclei were investigated under RR conditions. When the signal from the CTC of half-integer quadrupolar nuclei under spin-locking condition provided by a low rf field and a high spinning speed $[\alpha=\omega_{\mathrm{rf}}^2/\omega_r\chi_Q\ll 1$, where $\chi_Q=e^2qQ/2S(2S-1)\hbar]$ is sampled stroboscopically at integer multiples of the rotor period, the quadrupolar broadening mechanism disappears under the dual rf-spinning modulations [Fig. 1(A)]. The side bands arise from the noncommutative property of the CTC with the rf Hamiltonian in the quadrupolar interaction frame. The center and side bands coincide with each other when the RR conditions $\omega_{\mathrm{rf}}=n\omega_r/(S+1/2)(n=1,2,\ldots)$ are satisfied and interestingly various interactions such as CSA, HTD, HMD (Fig. 2), and the second-order quadrupolar interactions are reintroduced by the mutual cancellation of spinning and rf modulations [Fig. 1(B)]. A recoupling by a double quantum mode of mixing at $\omega_{\mathrm{rf}}=n\omega_r/(2S+1)$ $(n=1,2,\ldots)$ was also implemented for a dipole-coupled pair of quadrupolar nuclei.[40] A similar mechanism can also be considered for a HTD pair involving quadrupolar nuclei when both *S* and *I* are irradiated simultaneously at $\omega_{\mathrm{rf}}^{I,S}=n\omega_r/(S+I+1)$ $(n=1,2,\ldots)$. Very recently we presented a series of three- dimensional experiments to recover the anisotropic interactions of half-integer quadrupolar nuclei in the presence of site-specific resolution by combining rotary resonance recouplings (R^3) at $\omega_{\mathrm{rf}}=\omega_r/(2S+1)$ for HMD and $\omega_{\mathrm{rf}}=n\omega_r/(S+1/2)$ $(n=1,2)$ for CSA with the MQMAS experiment.[41]

This paper demonstrates experimental evidence and a theoretical framework incorporating an average Hamiltonian theory (AHT) to explain various recouplings involving quadrupolar nuclei under various RR conditions. Also presented are numerical calculations for the purpose of quantitative comparisons with the experimental spectra. We are currently exploring a bimodal-Floquet theory[42] for a quantitative description of these phenomena as was used for the description of FASTER MQMAS.[39]

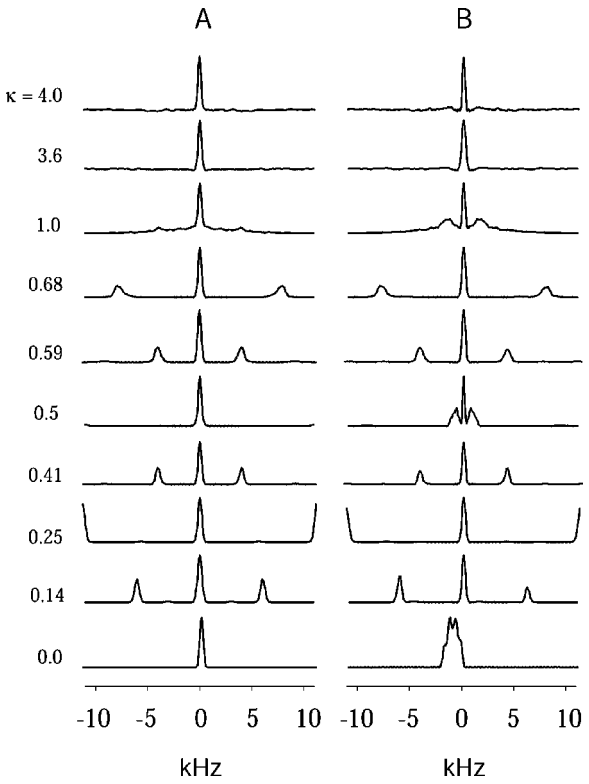

FIG. 1. Behavior of the central transition coherence of $S=3/2$ quadrupolar nucleus when sampled stroboscopically at integer multiples of the rotor period under spin locking $(\alpha=\omega_{\mathrm{rf}}^2/\omega_r\omega_Q\ll 1)$ and/or rotary resonance conditions $\kappa=\omega_{\mathrm{rf}}/\omega_r=n/2$ $(n=1,2)$ provided by rf spinning dual modulations. (A) The influence of the first-order quadrupolar interaction shows a center peak and two side bands. The side bands disappear at $\kappa=0.5$ and 1. (B) The second-order quadrupolar interaction adds its reintroduced line shape at rotary resonance conditions ($\kappa=1/2$, 1). The $n=1$ mode of the second-order quadrupolar interaction ($\kappa=1/2$) has a well defined and narrower line shape than that for higher *n*. Notice the usual 1D MAS line shapes in both cases when no rf field is applied during the evolution of central transition coherence ($\kappa=0$). The parameters used in the simulation are $\omega_0/2\pi=160$ MHz, $e^2qQ/2\pi h=2.5$ MHz, $\eta_Q=0.5$, $\omega_r/2\pi=22$ kHz. $20\times20\times20$ crystallite orientations together with 0.36 μs of time increment were incorporated in the simulation.

II. THEORETICAL

The reintroduction of CSA, dipolar couplings (both HTD and HMD), and the second-order quadrupolar interaction is demonstrated in systems involving half-integer quadrupolar nuclei under RR conditions induced by fast spinning and weak rf fields (Ref. 52). Throughout this work rotor synchronized pulses and stroboscopic detection at integer multiples of the rotor period are assumed. The spinning frequency is fast enough compared to the CSA or dipolar coupling strengths, and the rf-field strength is less than or equal to the spinning speed so that efficient RR or spin-locking condi-

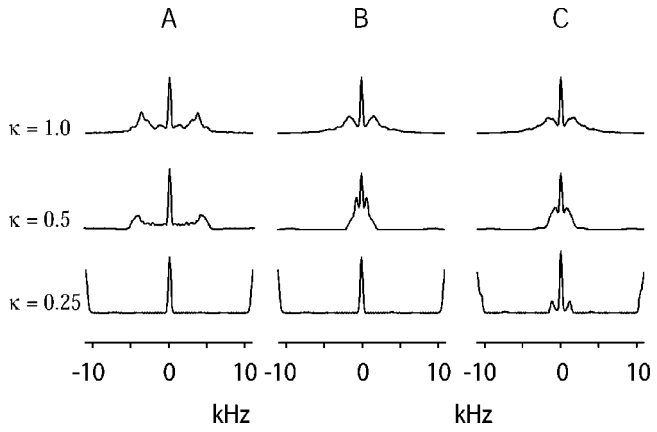

FIG. 2. Recouplings of CSA ($S=3/2$) (A), HTD ($S=3/2$, $I=1/2$) (B) and HMD ($S=I=3/2$) (C) at various rotary resonance conditions when the S nucleus is observed. Note the HMD's additional recoupling at $\kappa=0.25$ in terms of double quantum mode of coherence transfer between CTCs of S and I nuclei. The parameters used in the simulations are $\delta_{cs}=100$ ppm, $\eta_{cs}=0$, and $D_{zz}/2\pi=2.5$ kHz. Coinciding tensor orientations were assumed in all the simulations. All other parameters are the same as in Fig. 1.

tions ($\alpha=\omega_{\rm rf}^2/\omega_r\chi_Q\ll 1$) of the CTC of half-integer quadrupolar nuclei are fulfilled.[38–40] A moderate range of quadrupolar coupling constants are assumed so that the MAS scaled second-order quadrupolar anisotropy is smaller than the spinning speed.

A. Brute-force calculation

For a dipolar pair of a half-integer quadrupolar S nucleus coupled to an I nucleus (1/2 or any half-integer quadrupolar nucleus) under MAS and rf field irradiation, ignoring the indirect coupling term, the total Hamiltonian for the S spin is

$$H_s(t)=H_Q^{(1)}(t)+H_Q^{(2)}(t)+H_{CS}(t)+H_D(t)+H_{\rm rf}. \tag{1}$$

$H_Q^{(1)}(t)$ and $H_Q^{(2)}(t)$ are the first- and the second-order quadrupolar interactions given by

$$H_Q^{(1)}(t)=\chi_Q R_{2,0}^Q(t)\{3S_z^2-S(S+1)\} \tag{2}$$

and

$$H_Q^{(2)}(t)=\frac{3\chi_Q^2}{\omega_0}S_z[R_{2,-1}^Q(t)R_{2,1}^Q(t)\{4S(S+1)-8S_z^2-1\} + R_{2,-2}^Q(t)R_{2,2}^Q(t)\{2S(S+1)-2S_z^2-1\}], \tag{3}$$

respectively, where $\chi_Q=e^2qQ/2S(2S-1)\hbar$.

$H_{CS}(t)$ and $H_D(t)$ represent the chemical shift and dipolar interaction terms given by

$$H_{CS}(t)=\omega_0(\delta_{\rm iso}+\delta_{cs}R_{2,0}^{CS}(t))S_z \tag{4}$$

and

$$H_D(t)=R_{2,0}^D(t)(2I_zS_z-\tfrac{1}{2}(I_+S_-+I_-S_+)), \tag{5}$$

respectively. In the case of heteronuclear dipolar coupling, the flip–flop terms of Eq. (5) can be dropped. The radio-frequency Hamiltonian $H_{\rm rf}$ in the rotating frame is defined by

$$H_{\rm rf}=\omega_{\rm rf}S_x. \tag{6}$$

The various spatial tensor components $R_{2,m}^{\lambda}(t)(\lambda=Q,CS,D)$, can be written from their principal value components as

$$R_{2,m}^{\lambda}(t)=\sum_{n=-2}^{2}\sum_{k=-2}^{2}D_{n,m}^2(\omega_r t,\theta_m,0^\circ)D_{k,n}^2(\alpha^\lambda,\beta^\lambda,\gamma^\lambda)\rho_{2,k}^{\lambda}, \tag{7}$$

where $D_{m,n}^2(x,y,z)$ denote Wigner rotation matrices and $\theta_m=\arctan(\sqrt{2})$.[5] The Euler angle set $\{\alpha^\lambda,\beta^\lambda,\gamma^\lambda\}$ relate λ's principal values to those defined in the rotor fixed axis system, and $\{\omega_r t,\theta_m,0^\circ\}$ transforms the rotor fixed axis frame to the laboratory frame where the experiment is performed. The principal value components for the various interactions can be defined as follows:

$$\rho_{2,0}^Q=\frac{1}{2},\quad \rho_{2,\pm1}^Q=0,\quad \rho_{2,\pm2}^Q=\frac{\eta_Q}{2\sqrt{6}}, \tag{8}$$

$$\rho_{2,0}^{CS}=\sqrt{\frac{3}{2}},\quad \rho_{2,\pm1}^{CS}=0,\quad \rho_{2,\pm2}^{CS}=\frac{\eta_{cs}}{2}, \tag{9}$$

$$\rho_{2,0}^D=-\frac{2\hbar\gamma_I\gamma_S}{r_{IS}^3}=D_{zz},\quad \rho_{2,\pm1}^D=\rho_{2,\pm2}^D=0. \tag{10}$$

The evolution of the density matrix of CTC S_x^{2-3} ($S=3/2$), which is the observable of interest, can be obtained by solving the Liouville–von Neuman equation to give

$$\langle S_x^{2-3}\rangle={\rm Tr}\{U(t)S_x^{2-3}U^\dagger(t)S_x^{2-3}\} \tag{11}$$

with

$$U(t)=T\ \exp\left(-i\int_0^t H_s(t')dt'\right), \tag{12}$$

where T is the Dyson time-ordering operator. Equation (11) provides the exact numerical solution of the CTC's spin dynamics for an S spin under MAS and rf irradiation. Under a low rf field and high spinning conditions (i.e., $\alpha\ll 1$), the CTC is effectively spin locked. When the spin-locked CTC is sampled after each rotor period, the time-dependent first-order quadrupolar Hamiltonian shows a sharp center peak and a set of two side bands as demonstrated in Fig. 1. The side bands, which vary their positions depending on the ratio of $\kappa=\omega_{\rm rf}/\omega_r$, are induced by the interference of CT with the satellite transitions because S_x^{2-3} does not commute with $H_{\rm rf}$ in the quadrupolar interaction frame (see Sec. II B 1). The MAS nonvanishing fourth-rank term of the second-order quadrupolar interaction also acquires sinusoidal rf modulations in addition to the spinning modulations, and is therefore, averaged to zero when sampled stroboscopically at integer multiples of the rotor period [Fig. 1(B)].

When $\kappa=n/(S+1/2)$ ($n=1,2,\ldots$) the side bands coincide with the center peak while presenting the reintroductions of various couplings such as the second-order quadrupolar interaction [Fig. 1(B)], CSA [Fig. 2(A)], HTD [Fig. 2(B)], and HMD [Fig. 2(C)] in the Fourier modes of n

$=1,2,\ldots$. A part of the CTC is also transferred to MQC at $n=2,4,\ldots$ modes, which has been exploited for efficient MQC preparation in MQMAS.[38]

In the case of a homonuclear quadrupolar spin pair, additional recoupling conditions occur at $\kappa=n/(2S+1)$ ($n=1,2,\ldots$) due to the double quantum modes of coherence transfers between two quadrupolar nuclei within the CTC's subspace [Fig. 2(C)]. As will be shown in Sec. III C, another double quantum mode of recoupling mechanism applicable for a heteronuclear spin pair is expected at $\kappa=n/(I+S+1)$ ($n=1,2,\ldots$) when both I ($\geqslant 1/2$) and S channels are irradiated simultaneously [e.g., when $I=1/2$ and $S=3/2$, $\omega_{\mathrm{rf}}^{S}=\omega_{\mathrm{rf}}^{I}=\omega_r/3$ satisfies $(S+1/2)\omega_{\mathrm{rf}}^{S}+(I+1/2)\omega_{\mathrm{rf}}^{I}=\omega_r$]. In these inter-nuclear double quantum modes of recoupling conditions, however, leakage of CTC to MQC within a single nucleus can be prevented. These modes are applicable to both HMD and HTD couplings, and can be exploited selectively in quadrupolar spin systems.

An analytical expression based on the bimodal Floquet theory[42] may be required in order to understand all the recoupling characteristics under RR conditions since the various internal Hamiltonians should be expanded in Fourier modes of both ω_{rf} and ω_r. In this paper, however, we have incorporated an average Hamiltonian theory (AHT)[5] which provides useful insight into the rotary resonance recouplings of half-integer quadrupolar nuclei.

B. Average Hamiltonian treatments

1. Recouplings at $\kappa=n/(S+1/2)$ ($n=1,2$)

In order to illustrate the recouplings of the various interactions at RR conditions, the simple case of an $S=3/2$ is examined. For an S nucleus in an isolated environment or in a dipolar pair S–I, the total Hamiltonian provided by Eqs. (1)–(6) can be rewritten in terms of the fictitious spin-1/2 formalism as[43]

$$H_s(t)=H_Q^{(1)}(t)+H_\Omega(t)+H_{\mathrm{rf}}, \tag{13}$$

where $H_Q^{(1)}(t)$ is the dominant first-order quadrupolar interaction defined by

$$H_Q^{(1)}(t)=\omega_Q(t)(S_z^{1-2}-S_z^{3-4}). \tag{14}$$

$H_\Omega(t)$ represents a shiftlike Hamiltonian, a sum of the chemical shift, heteronuclear dipolar interaction, and second-order quadrupolar interaction, provided by

$$H_\Omega(t)=\{\Omega_{CS}^{2-3}(t)+\Omega_D^{2-3}(t)I_z+\Omega_Q^{2-3}(t)\}S_z^{2-3}+\{\Omega_{CS}^{-4}(t)+\Omega_D^{1-4}(t)I_z+\Omega_Q^{1-4}(t)\}S_z^{1-4}. \tag{15}$$

H_{rf} is the radio-frequency Hamiltonian given by

$$H_{\mathrm{rf}}=\omega_{\mathrm{rf}}\{2S_x^{2-3}+\sqrt{3}(S_x^{1-2}+S_x^{3-4})\}. \tag{16}$$

The dominant first-order quadrupolar term can be removed by transforming Eqs. (14)–(16) into the quadrupolar interaction frame defined as[33,39,40]

$$\tilde{H}_s=U_Q^{\dagger}\,H_s\,U_Q, \tag{17}$$

where $U_Q=T\,\exp(i\int_0^t\omega_Q(t')dt'(S_z^{1-2}-S_z^{3-4}))$.

Since the shift Hamiltonian, Eq. (15) commutes with $H_Q^{(1)}(t)$ at all times,

$$\tilde{H}_\Omega(t)=H_\Omega(t). \tag{18}$$

The rf Hamiltonian in the quadrupolar interaction frame will be[39,40]

$$\tilde{H}_{\mathrm{rf}}(t)=\omega_{\mathrm{rf}}\Bigg(2S_x^{2-3}+\sqrt{3}\Bigg((S_x^{1-2}+S_x^{3-4})\times\cos\Bigg(\int_0^t\omega_Q(t')dt'\Bigg)+(S_y^{1-2}-S_y^{3-4})\sin\Bigg(\int_0^t\omega_Q(t')dt'\Bigg)\Bigg)\Bigg). \tag{19}$$

When the CTC is effectively spin-locked ($\alpha\ll 1$) and away from RR conditions, one can safely ignore the time dependent terms which connect the CTC to other coherences from Eq. (19) as justified by Baldus *et al.*[40] When a qualitative picture for the recouplings of $\Omega_\lambda^{2-3}(t)$ ($\lambda=CS,D,Q$) is desired, this assumption can be extended further to the RR conditions because the reintroduction of couplings at the RR conditions take place in the CTC. Moreover, as long as we are dealing with recouplings within the CTC's subspace, the terms representing $3Q$ coherence $\Omega_\lambda^{1-4}(t)$ in Eq. (15) can also be dropped. The effective terms of the Hamiltonian governing the recoupling within the CTC are

$$\tilde{H}_t^{CT}(t)=\{\Omega_{CS}^{2-3}(t)+\Omega_D^{2-3}(t)I_z+\Omega_Q^{2-3}(t)\}S_z^{2-3}+2\omega_{\mathrm{rf}}S_x^{2-3}, \tag{20}$$

with

$$\Omega_{CS}^{2-3}(t)=\sum_{m=-2}^{2}\omega_{CS}^{m}(\alpha^{CS},\beta^{CS})\exp(im(\gamma^{CS}+\omega_r t)), \tag{21}$$

$$\Omega_D^{2-3}(t)=\sum_{m=-2,m\neq 0}^{2}\omega_D^{m}(\beta^{D})\exp(im(\gamma^{D}+\omega_r t)), \tag{22}$$

and

$$\Omega_Q^{2-3}(t)=\frac{3}{\omega_0}\chi_Q^2[4S(S+1)-3]\times\sum_{m=-4}^{4}\omega_Q^{m}(\alpha^{Q},\beta^{Q})\exp(im(\gamma^{Q}+\omega_r t)). \tag{23}$$

The expressions of $\omega_{CS}^{m}(\alpha^{CS},\beta^{CS})$ and $\omega_D^{m}(\beta^{D})$ can be found elsewhere,[9,11] and the explicit forms of $\omega_Q^{m}(\alpha^{Q},\beta^{Q})$ are provided in the Appendix.

In a toggling frame defined by an operator

$$\exp(i2\omega_{\mathrm{rf}}t\cdot S_x^{2-3})=\exp\Bigg(-i\frac{\pi}{2}S_y^{2-3}\Bigg)\exp(i2\omega_{\mathrm{rf}}t\cdot S_z^{2-3})\times\exp\Bigg(i\frac{\pi}{2}\cdot S_y^{2-3}\Bigg), \tag{24}$$

the CTC's effective spin-locking Hamiltonian becomes[11,40]

$$k_\lambda \Omega_\lambda^{2-3}(t)\{S_x^{2-3}\cos(2\omega_{\rm rf}t)+S_y^{2-3}\sin(2\omega_{\rm rf}t)\}$$
$$=k_\lambda \Omega_\lambda^{2-3}(t)\{S_+^{2-3}e^{-2i\omega_{\rm rf}t}+S_-^{2-3}e^{2i\omega_{\rm rf}t}\}, \quad (25)$$

where $k_{CS}=k_Q=1$ and $k_D=I_z$. At the RR conditions, $\omega_{\rm rf}=n\omega_r/2$,

$$\omega_{CS}^{\pm n}(\alpha^{CS},\beta^{CS})e^{\pm in\gamma^{CS}} \quad (26)$$

for the CSA,

$$I_z\omega_D^{\pm n}(\beta^D)\, e^{\pm in\gamma^D} \quad (27)$$

for the heteronuclear dipolar interaction, and

$$\frac{3}{\omega_0}\chi_Q^2[4S(S+1)-3]\cdot\omega_Q^{\pm n}(\alpha^Q,\beta^Q)e^{\pm in\gamma^Q} \quad (28)$$

for the second-order quadrupolar interaction will be reintroduced. When $n=1$ and $n=2$, the CSA, HTD, and the second-order quadrupolar interaction all lose their time dependence at $\kappa=0.5$ and $\kappa=1$, respectively. The angle $\gamma^\lambda(\lambda=CS,D,Q)$ affects only the phase and not the amplitude; therefore, only the amplitude of each recoupling, $2\Gamma^\lambda|\omega_\lambda^{\pm n}|$, will be provided, where $\Gamma^{CS}=\Gamma^D=1$ and $\Gamma^Q=3\chi_Q^2[4S(S+1)-3]/\omega_0$.

The CSA recoupling at $\kappa=0.5$ ($n=1$) has a cancellation effect with respect to the second-order quadrupolar recoupling because of the negative sign in front of the real part of the $n=1$ CSA term:

$$\left|\frac{\chi_Q^2}{4\sqrt{2}\omega_0}[4S(S+1)-3]\left(\frac{BD}{4}-\frac{AB}{2}-\frac{CE}{9}\right)\right.$$
$$-\frac{\omega_0\delta_{cs}}{\sqrt{2}}\sin 2\beta^{cs}\left(1-\frac{\eta_{cs}}{3}\cos 2\alpha^{cs}\right)$$
$$\pm i\frac{3\chi_Q^2}{2\sqrt{2}\omega_0}[4S(S+1)-3](BE+CD-6AC)$$
$$\left.+\frac{\sqrt{2}\omega_0\delta_{cs}\eta_{cs}}{3}\sin\beta^{cs}\sin 2\alpha^{cs}\right|, \quad (29)$$

where the definitions of A, B, C, D, and E are given in the Appendix. Therefore, when $\delta_{cs}>0$, an increase of CSA decreases the recoupling line width expected from the second-order quadrupolar interaction until a certain point which is determined by the relative magnitudes of two couplings. A further increase of CSA results in a constant increase of recoupled spectral width as demonstrated in Fig. 3(A). When $\delta_{cs}<0$ the influence of CSA just adds up to the width obtained by the second-order interaction [Fig. 3(B)]. This fact may cause some ambiguity assigning a CSA value from the experimental spectrum of unknown quadrupolar and CSA parameters due to the existence of other possible sets of values. Another recoupling measurement at $\kappa=1$, however, removes this ambiguity based on the distinct line shapes of different CSA values which give identical linewidths at $\kappa=0.5$. In this manner, not only the magnitude but also the sign of CSA interaction of half-integer quadrupolar nucleus can be obtained when both the recoupled spectra at $\kappa=0.5$ and 1 are compared. However, the sign of the quadrupolar interaction still cannot be determined because of its quadratic dependence.[19]

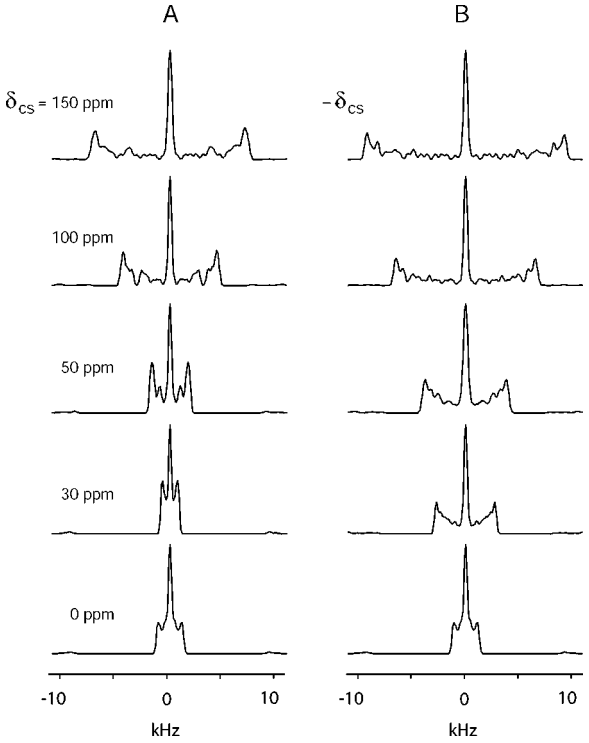

FIG. 3. Comparisons of the recoupled line shapes coming from different signs of CSA at $\kappa=0.5$. As predicted in Eq. (29), a cancellation between CSA and the second-order quadrupolar interaction is evident when $\delta_{cs}>0$ (A) and an additive behavior between them when $\delta_{cs}<0$ (B). Collinear CSA and quadrupolar tensors were assumed. Parameters used in the simulation: $S=3/2$, $\omega_0/2\pi=160$ MHz, $e^2qQ/2\pi\hbar=2.5$ MHz, $\eta_Q=0.5$, $\omega_r/2\pi=22$ kHz. $25\times25\times25$ crystallite orientations together with 0.36 μs of time increment were incorporated in the simulation.

2. Recouplings of dipolar interactions using a double quantum mode

In the simplest case of $S=I=3/2$, the HMD interaction has a unique recoupling condition at $\kappa=0.25$ which provides its selective reintroduction at $n=1$ mode as represented in Fig. 2(C). Generally, the underlying principle applicable to the HMD interaction at $\kappa=n/(2S+1)$ ($n=1,2,\ldots$) involves a double quantum mode coherence transfer between the CTCs of half-integer quadrupolar nuclei. For a $S=I=3/2$ HMD pair, by using the definition of angular momentum operators:

$$F_x=\sqrt{3}(F_x^{1-2}+F_x^{3-4})+2F_x^{2-3},$$
$$F_y=\sqrt{3}(F_y^{1-2}+F_y^{3-4})+2F_y^{2-3}, \quad (30)$$
$$F_z=3F_z^{1-4}+F_z^{2-3}$$

with $F=I,S$, the dipolar Hamiltonian, Eq. (5), can be rewritten as[40]

$$H_{\mathrm{HMD}}^{2-3}(t)=2\sum_{n=-2,n\neq 0}^{2}\omega_D^{\pm n}(\beta^D)e^{\pm in(\omega_r t+\gamma^D)}\times(I_z^{2-3}S_z^{2-3}-2I_x^{2-3}S_x^{2-3}-2I_y^{2-3}S_y^{2-3}), \tag{31}$$

where

$$\omega_D^{\pm 1}=-\frac{D_{zz}}{4\sqrt{2}}\sin 2\beta^D, \tag{32}$$

$$\omega_D^{\pm 2}=\frac{D_{zz}}{8}\sin^2\beta^D. \tag{33}$$

A tilted frame with $\omega_{F,\mathrm{eff}}=\sqrt{\Omega_{F,CS,Q}^2+(2\omega_{\mathrm{rf}})^2}$ ($F=I$ or S) along a new z axis can be postulated as[40,44]

$$\begin{aligned}\tilde{F}_z^{2-3}&=\cos\theta_F F_z^{2-3}+\sin\theta_F F_x^{2-3},\\ \tilde{F}_x^{2-3}&=-\sin\theta_F F_z^{2-3}+\cos\theta_F F_x^{2-3},\\ \tilde{F}_y^{2-3}&=F_y^{2-3}\end{aligned} \tag{34}$$

with $\theta_F=\arctan(2\omega_{\mathrm{rf}}/\Omega_{F,CS,Q})$. A transformation into an interaction frame defined by

$$\exp(i\omega_{S,\mathrm{eff}}\tilde{S}_z^{2-3}t)\exp(i\omega_{I,\mathrm{eff}}\tilde{I}_z^{2-3}t) \tag{35}$$

yields a double-quantum dipolar expression

$$\tilde{H}_{\mathrm{HMD}}^{2-3}(t)=Q(\theta_I,\theta_S)\sum_{n=-2,n\neq 0}^{2}\omega_D^{\pm n}e^{\pm in(\omega_r t+\gamma^D)}\times(\tilde{I}_+^{2-3}\tilde{S}_+^{2-3}e^{-i(\omega_{I,\mathrm{eff}}+\omega_{S,\mathrm{eff}})t}+\tilde{I}_-^{2-3}\tilde{S}_-^{2-3}e^{i(\omega_{I,\mathrm{eff}}+\omega_{S,\mathrm{eff}})t}) \tag{36}$$

with $Q(\theta_I,\theta_S)=(1-2\cos\theta_I\cos\theta_S+2\sin\theta_I\sin\theta_S)$.

When $\theta_S=\theta_I=90°$ (i.e., $\Omega_{F,CS,Q}=0$), a double-quantum mode of dipolar recoupling

$$3\omega_D^{\pm n}(\beta^D)e^{\pm in\gamma^D} \tag{37}$$

will be established at the $\kappa=\omega_{\mathrm{rf}}/\omega_r=n/4$ conditions. Since γ^D angle does not influence the recoupling amplitude, the $2Q$ nutation frequency will be given as $3D_{zz}\sin 2\beta^D/4\sqrt{2}$ for $n=1$ and $3D_{zz}\sin^2\beta^D/8$ for $n=2$ as in the cases of the *2Q*-HORROR method applied to homonuclear dipolar pair of spin-1/2 system.[14]

In a close analogy to the homonuclear case, the double quantum mode of dipolar recoupling can be implemented also for the heteronuclear dipolar interactions, when both S and I channels are being irradiated at $\kappa=n/(S+I+1)$. In the simplest case of $S=3/2$ and $I=1/2$ the effective HTD Hamiltonian in a toggling frame defined by

$$\exp(2i\omega_{\mathrm{rf}}t\cdot S_z^{2-3})\exp\left(i\frac{\pi}{2}S_y^{2-3}\right)\exp(i\omega_{\mathrm{rf}}t\cdot I_z)\exp\left(i\frac{\pi}{2}I_y\right) \tag{38}$$

will be

$$\sum_{n=-2,n\neq 0}^{2}\omega_D^{\pm n}(\beta^D)e^{in(\omega_r t+\gamma^D)}\times(S_+^{2-3}I_+e^{-3i\omega_{\mathrm{rf}}t}+S_-^{2-3}I_-e^{3i\omega_{\mathrm{rf}}t}). \tag{39}$$

The double quantum mode of recoupling, at integer multiples of $\omega_r/3$, is $D_{zz}\sin 2\beta^D/4\sqrt{2}$ for $n=1$, and $D_{zz}\sin^2\beta^D/8$ for $n=2$. The selective nature of double quantum mode is a promising method to measure the distance between two spins involving one or two quadrupolar nuclei.

III. EXPERIMENTAL IMPLEMENTATIONS

The rotary resonance recoupling for the various interactions in half-integer quadrupolar nuclei discussed above were shown experimentally in ^{23}Na-, ^{87}Rb-, and ^{11}B-NMR using anhydrous Na_2SO_4, Rb_2CrO_4 and bis(pinacolato)diboron (BPDB). All the nuclei are $S=3/2$, and the compounds have known quadrupolar parameters.[45–47] The homonuclear dipolar coupling of BPDB is $D_{zz}/2\pi=2.5$ kHz.[48] The spectra were measured at 11.7 T using a Varian/Chemagnetics Infinity spectrometer with commercial 3.2 mm and 4 mm Chemagnetics probes spinning at 20 kHz and 16 kHz, respectively.

A. Calibration of the rotary resonance conditions of half-integer quadrupolar nuclei

To identify the rf intensities that match the rotary resonance conditions, a 90° pulse followed by a spin-locking pulse fixed at integer multiples of the rotor period was implemented while sweeping the *rf* intensities [Fig. 4(A)].[40] An example of spin-locking and the various RR conditions at $\kappa=1/4$, 1/2, and 1 in the BPDB sample is provided in Fig. 4(b). Here, the central transition of ^{11}B nuclei was spin locked for eight rotor periods and monitored as a function of applied rf field intensities. As can be seen in Fig. 4(B), local minima at 5 kHz ($\kappa=1/4$), 10 kHz ($\kappa=1/2$), and 20 kHz ($\kappa=1$) with 20 kHz MAS spinning frequency are identified. The $\kappa=n/4$ ($n=1,2,\ldots$) conditions are responsible for the double quantum mode coherence transfer between the CTCs of the two ^{11}B nuclei based on the HMD coupling. Additionally, at the $\kappa=n/2$ ($n=1,2,\ldots$) conditions, RR recoupling occurs under the single quantum mode for the CSA and second-order quadrupolar interactions. At the conditions $\kappa=n/2$ ($n=1,2,\ldots$) recoupling of the CTC to TQC occurs also, reducing the spin lock efficiency.[39] The actual rf intensities were also compared to the value obtained from 90° pulse length in a liquid sample.

B. Measurements of CSA and heteronuclear dipolar interaction of half-integer quadrupolar nucleus

A two-dimensional version of the pulse sequence [Fig. 4(A)] (a similar type of this pulse sequence was used in the spin-1/2 system for the recoupling of the CSA and dipolar interactions[11,14]) was adopted to observe the recouplings operating at the $\kappa=n/2$ ($n=1,2$) conditions. The spin-locking periods after the 90° pulse were incremented in the indirect dimension by integer multiples of the rotor periods before acquiring the signal under free precession. The resulting 2D spectrum contains a normal MAS quadrupolar line shape

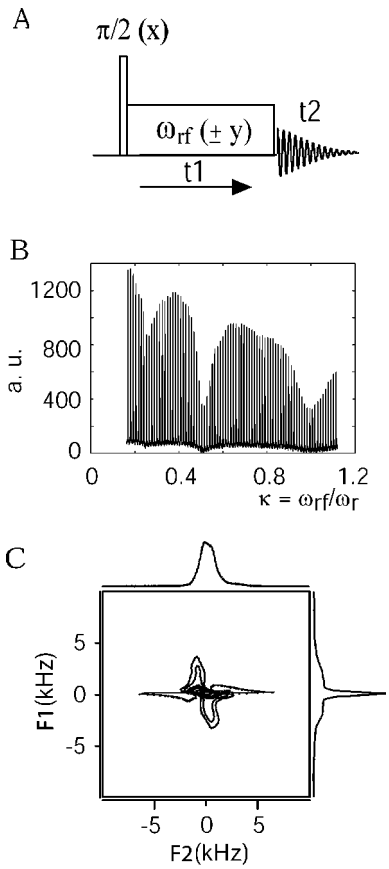

FIG. 4. Experimental scheme used for the recoupling of various interactions involving half-integer quadrupolar nuclei ($S=I=3/2$). ^{11}B NMR at 11.7 T magnetic field was performed at bis(pinacolato)diboron, $B_2C_{12}O_4H_{24}$ (BPDB). (A) The pulse sequence. (B) A calibration profile of ^{11}B NMR spectra measured on BPDB as a function of rf field intensity by fixing the τ_1 spin-locking time at $8\tau_r$ under a fast speed sample spinning (20 kHz). Note the characteristic local minima observed at 5, 10, and 20 kHz of rf field intensities which corresponding to $\kappa=0.25$, 0.5, and 1, respectively. (C) A 2D ^{11}B NMR recoupling experiment measured on BPDB at $\kappa=0.5$. Stroboscopic sampling at integer multiples of τ_r was used in both time domains. The direct sampling domain has a normal 1D MAS spectrum while the projected spectrum along indirect domain contains recoupled information.

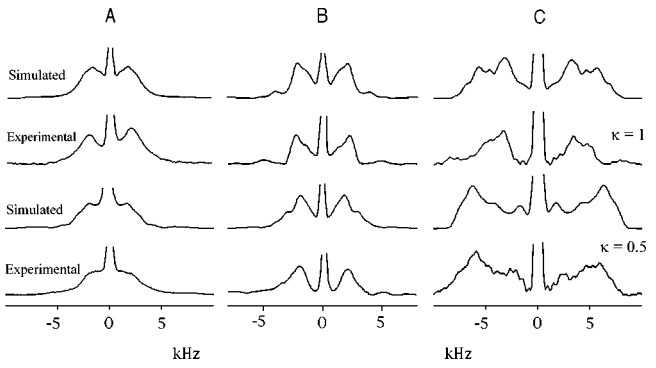

FIG. 5. Comparisons between experimentally measured and simulated spectra at $\kappa=0.5$ and 1 on (A) BPDB, (B) anhydrous sodium sulfate, and (C) rubidium chromate. The influences of the second-order quadrupolar interaction in both κ values were estimated based on the 1D MAS spectra and brute force simulations; BPDB (Ref. 45): $e^2qQ/2\pi\hbar=2.5$ MHz, $\eta_Q=0.3$; Na_2SO_4 (Ref. 46), $e^2qQ/2\pi\hbar=2.6$ MHz, $\eta_Q=0.6$; Rb_2CrO_4 (Ref. 47), $e^2qQ/2\pi\hbar=3.5$ MHz, $\eta_Q=0.3$ (the second rubidium site is not considered here)). The magnitude of CSA of ^{11}B nuclei in BPDB and ^{87}Rb in rubidium chromate were about 50 ppm and -100 ppm, respectively. The coinciding CSA and quadrupolar tensors for BPDB and the relative orientations of {0°,70°,0°} between the two tensors for rubidium chromate provided the best matchs. The sodium nuclei of Na_2SO_4 have negligible CSA value (<20 ppm) and the experimental spectra at $\kappa=0.5$ and 1 were simulated only by the second-order quadrupolar effect. The influence of HMD interaction at $\kappa=1/2$ was ignorable even in the case of BPDB due to its much smaller order of magnitude compared to CSA or the second-order quadrupolar interactions.

along the direct domain and a recoupled spectrum along the indirect domain. Fig. 4(C) shows an example of a 2D spectrum measured on the BPDB sample at $\kappa=1/2$.

Projections along the indirect domain of the experimentally measured 2D spectra and the corresponding best fit simulations of the BPDB, sodium sulfate and rubidium chromate at $\kappa=1/2$ and $\kappa=1$ conditions are given in Figs. 5(A), 5(B), and 5(C), respectively. Since the contributions of the second-order quadrupolar interaction and the |HMD| interaction can be estimated from the 1D MAS spectrum and x- ray data, respectively, the determination of the CSA's contribution in the recoupled spectra was possible. The $\kappa=1/2$ condition is preferable over the $\kappa=1$ due to the less broadened recoupled second-order quadrupolar linewidth [Fig. 1(B)] despite the mutual cancellation effect. This fact is also true for the recouplings of HTD and HMD interactions at the $\kappa=n/(S+1/2)$ modes. The influences of the second-order quadrupolar interactions at $\kappa=1/2$ are 2.6 kHz for BPDB, 3.2 kHz for Na_2SO_4 and 4.1 kHz for Rb_2CrO_4 as estimated from Eq. (28) and brute-force calculations (BPDB,[45] $e^2qQ/2\pi\hbar=2.5$ MHz, $\eta_Q=0.3$; Na_2SO_4,[46] $e^2qQ/2\pi\hbar=2.6$ MHz, $\eta_0=0.6$; Rb_2CrO_4[47] $e^2qQ/2\pi\hbar=3.5$ MHz, $\eta_0=0.3$). The $n=2$ mode of HMD recoupling at $\kappa=1/2$ was ignored in the case of Na_2SO_4 and Rb_2CrO_4, and 938 Hz in BPDB from the known bond distance.[48] Exact simulations based on brute-force calculation provided 50 ppm and -110 ppm of CSA in BPDB and rubidium chromate, respectively. Coinciding relative tensor orientations between the quadrupolar and CSA interactions were inferred from BPDB and $\{\alpha,\beta,\gamma\}=\{0°,70°,0°\}$ angle set between the two tensors provided the best fit simulation for Rb_2CrO_4.[47] The second-order quadrupolar interaction alone explains most of the features of recoupled spectra in Na_2SO_4. Based on the exact simulation, the CSA of Na_2SO_4 is less than 20 ppm. It is noteworthy that this RR recoupling method enables the observation of a rather small CSA in a quadrupolar spin system which has a quadrupolar coupling constant of several MHz.

C. Recoupling of dipolar interactions in double-quantum mode

A selective recoupling of the dipolar interactions involving quadrupolar nuclei can be realized when a double-quantum mode of mixing is utilized. In the simplest case of a half-integer homonuclear pair $S=I=3/2$, when a mixing pulse with $\kappa=1/4$ is carried out on the F_z ($F=S,I$) magnetization before applying a 90° reading pulse, an HMD Pake pattern can be obtained selectively along the indirect domain. This is similar to the double quantum mode of recoupling applied for a homonuclear spin-1/2 system[14] except for the fact that here the equilibrium state of F_z was directly used for the mixing. Figure 6(A) shows a pulse sequence adopted

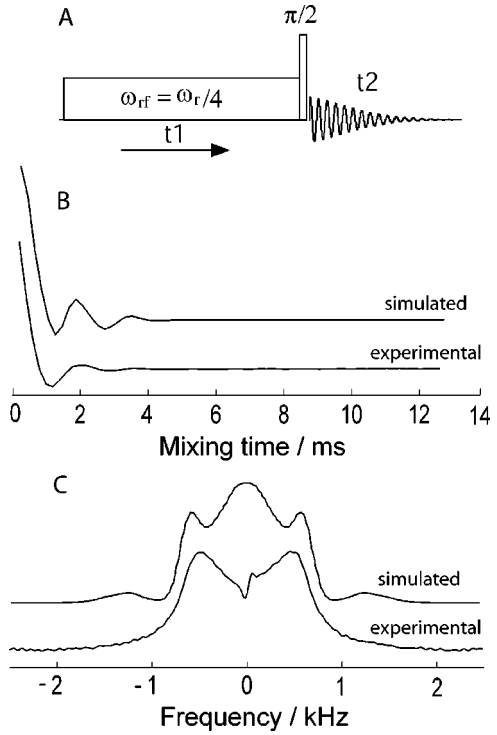

FIG. 6. Comparisons between experimentally measured and simulated double quantum mode homonuclear dipolar recoupling of the $^{11}B-^{11}B$ pair in BPDB sample at 11.7 T. A longitudinal mixing pulse at $\kappa=0.25$ was incremented by $4\tau_r$ in the indirect dimension before a 90° reading pulse was applied (A). The experimentally measured and simulated time domain spectra along t_1 (B) and their Fourier transforms into frequency domain after DC correction (C) are compared. The 2.5 kHz [$r(^{11}B-^{11}B)=1.7$ Å] (Ref. 48) of HMD coupling strength compares well with the experimental ~1.3 kHz width of the Pake-type pattern which can also be predicted by AHT. The simulated dipolar double quantum decay signal has a line broadening factor of 200 Hz. The wiggling features outside of the CTC's Pake-type pattern may come from a higher-order effect or an influence of the satellite transitions.

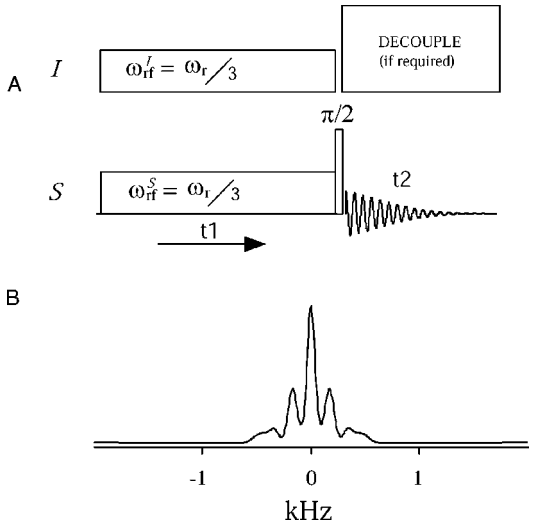

FIG. 7. A double quantum mode of HTD recoupling expected when both S and I channels are irradiated simultaneously at $\kappa=n/(S+I+1)$ ($n=1,2$). The signal along the indirect domain should be sampled at every $(S+I+1)\tau_r$. The spectrum shows a double quantum mode of recoupling of HTD pair of $S=3/2$ and $I=1/2$ having 2 kHz of dipolar coupling. The other parameters used in the simulation are $(e^2qQ/2\pi\hbar)_S=2.5$ MHz, $\eta_Q^S=0.3$, $\omega_r/2\pi=20$ kHz.

for this purpose. Mixing at the equilibrium state followed by a 90° pulse encodes a time signal based on the double quantum mode of pure HMD interaction along the indirect domain t_1. The indirect domain has to be incremented by four rotor periods to only observe the double-quantum mode of dipolar oscillations. A DC offset correction may be needed to remove the uninteresting sharp peak at zero frequency due to the uniform elevation of an indirect 1D FID signal along t_1 formed on each MAS spectrum obtained by the Fourier transformation along the direct time domain t_2. An offset difference also affects the characteristic features of spectrum observed as can be inferred from Eq. (36). In the experiment, the rf pulse was on resonance which provides the best condition for the double quantum mode of mixing.

Figures 6(B) and 6(C) show, respectively, the decay signal of the pure homonuclear dipolar interaction in the double quantum mode (the slices covering the MAS scaled second-order quadrupolar anisotropic line shape along the direct domain were summed) and its Fourier transformed spectrum measured on the BPDB sample. A simulated spectrum using the brute-force calculation was also provided in each case. The resulting simulated time domain signals were apodized using a exponential multiplication with 200 Hz line broadening. To our knowledge, this is the first example of pure dipolar Pake-type pattern for a homonuclear dipolar pair consisting of quadrupolar nuclei. The line width of ~1.3 kHz agrees well with the 2.5 kHz [$r(^{11}B-^{11}B)=1.71$ Å][48] of dipolar coupling strength based on the $3D_{zz}\sin 2\beta^D/4\sqrt{2}$ scaling factor available from AHT theory. When $\sin 2\beta^D=1$ the 2.5 kHz of dipolar strength provides 1325 Hz of magnitude of dipolar pattern which agrees well with the experiment. As was discussed earlier, the $\kappa=1/4$ condition is away from any other resonance conditions because there is no loss of CTC to MQC or the recouplings of CSA, second-order quadrupolar interaction, etc.

A double quantum mode of separation of the HTD interaction can also be realized by irradiating both the I and the S channels at $\kappa=n/(S+I+1)$ ($n=1,2$) as explained in the theory section. Figure 7(A) shows a pulse sequence for this purpose, and Fig. 7(B) shows the corresponding simulated spectrum incorporating $D_{zz}/2\pi=2$ kHz, $e^2qQ/2\pi\hbar=3$ MHz, $\eta_Q=0$ of a dipolar pair ($S=3/2$, $I=1/2$) by irradiating both channels at $\kappa=1/3$. Other conditions may also provide the double quantum mode of HTD recouplings as long as $(S+1/2)\omega_{\mathrm{rf}}^S+(I+1/2)\omega_{\mathrm{rf}}^I=\omega_r$ or $2\omega_r$ conditions are satisfied. Based on brute-force simulations, however, not all of conditions showed the desired Pake pattern due to their failure to provide a coincident peak pattern of side bands to the central peak. A selective HTD recoupling occurred on the side band peaks in all the cases, but if it did not coincide with the central peak, a complicated line shape not predictable by the simple AHT theory was obtained.

IV. DISCUSSION AND CONCLUSIONS

RR conditions provided by a low rf field and high spinning speed not only provide efficient MQC preparation but also reintroduce various interactions such as the CSA, dipo-

lar, and the second- order quadrupolar interactions which are otherwise averaged to zero or scaled down under MAS. The dual modulated nature of the spatial part of interactions under a spin-locking condition provided by a low rf field and high spinning condition ($\alpha \ll 1$) renders a possibility of removing the quadrupolar anisotropic line broadening from the line shapes. A part of CTC remained at $\kappa = n/(S+1/2)$ ($n = 1,2,\ldots$) is subject to make various recouplings such as the CSA, dipolar and the second-order quadrupolar interactions. When the CSA value involved in the quadrupolar nucleus is relatively small, this method provides a promising mechanism to evaluate the CSA parameters of a half-integer quadrupolar nucleus.

Among the two recoupling modes of rotary resonance conditions [$\kappa = n/(S+1/2)$ ($n=1,2$)] the first one, which uses $n=1$ Fourier index, provides a better condition due to its less broadened feature of the line shape although this mode shows a mutual cancellation effect with respect to the second-order quadrupolar interaction. However, neither of these modes is adequate for the measurements of HTD or HMD because of the nonselective nature among them as well as the dominating CSA and the second-order quadrupolar interactions.

A longitudinal mixing was used to build up a double quantum mode of coherence transfer between a dipolar pair involving quadrupolar nuclei. Double quantum modes of dipolar recoupling for HMD and HTD occur at $\kappa = n/(2S+1)$ ($n=1,2,\ldots$) and at $\kappa = n/(S+I+1)$ ($n=1,2,\ldots$), respectively. The required stroboscopic samplings along the recoupling domain should be implemented by every $(2S+1)\tau_r$ for HMD and $(S+I+1)\tau_r$ for HTD, respectively. The very selective nature of these double quantum modes of dipolar recoupling also contains the additional advantage of being able to occur away from RR conditions of losing CTC to MQC within a single nucleus. Both modes of double quantum dipolar recoupling have potential to be valuable tools to elucidate structures for nuclear spin systems involving quadrupolar nuclei. In contrast to the recoupling condition $\kappa = n/(2S+1)$ for the HMD case, the calibration of $\kappa = n/(S+I+1)$ for the HTD coupling is difficult because no local minimum can be observed when the quadrupolar S nucleus is considered alone. An iterative, trial-and-error method might be required to calibrate this resonance condition by irradiating both I and S channels.

Considering the facts that the relaxation in longitudinal mixing is T_1 limited rather than T_2 limited and that neither the second-order quadrupolar interaction nor the CSA is involved during the mixing evolution at $\kappa = n/(2S+1)$, or $\kappa = n/(S+I+1)$, these conditions may be exploited for samples containing dipolar pairs of quadrupolar nuclei with quadrupolar coupling constants in the range of several MHz. A solid echo type of measurement is also promising when it is used as a detection method. The double quantum mode of coherence transfer adopting a transverse mixing [pulse sequence of Fig. 4(A) type] was not successful even for the HMD recoupling at $\kappa = 1/4$ condition with BPDB sample which has a ^{11}B–^{11}B dipolar coupling of 2.5 kHz as shown in Fig. 2(C).

The linewidth of RR recoupling is a complicated function of the magnitudes, asymmetries, and relative orientations of the various tensors involved. The ambiguities can partially be relieved by the 1D MAS spectrum by determining the magnitude and asymmetry of quadrupolar interaction and by any x-ray diffraction data in order to determine the dipolar coupling strength if available. Simulations have demonstrated that the relative tensor orientations between quadrupolar and dipolar interaction are not so critical when a double quantum mixing of dipolar interaction is under consideration.

The recoupling linewidths of CSA, dipolar couplings, and the second-order quadrupolar interaction are well predicted by average Hamiltonian theory (AHT). However, in order to understand all of the spin dynamics at the RR conditions, a better method such as the bimodal-Floquet theory may be incorporated. Otherwise, a brute-force simulation must be carried out for a quantitative comparison to the experimental spectrum even though the AHT theory qualitatively explains all the recoupling conditions.

When a system consisting of many chemically and magnetically distinct sites is investigated, the pulse block of the R^3 has to be combined with the MQMAS experiment in order to have recoupling information on the top of site specific resolution.[41] A 3D version of this experiment is required to characterize not only the usual 2D MQMAS spectrum but also a recoupled spectrum of CSA or dipolar interactions of each site. A FASTER MQMAS method[38] combined into R^3 of dipolar interaction (both HTD or HMD) will have the full advantage of using the characteristics of half-integer quadrupolar nuclei under low rf field and high spinning speed in the sense that an efficient spin-locking, an effective double quantum coherence transfer, and an intense multiple quantum preparation and conversion can be incorporated.

When ^1H or ^{19}F are considered together with a half-integer quadrupolar nucleus, a new way of cross polarization (CP) under high spinning and low rf fields, based on the RR phenomenon operating in the zero- or double-quantum mode, is expected.[49–51] Our condition applied for the double quantum mode of heteronuclear dipolar recoupling satisfies one of these CP requirements because the rf fields of $I=1/2$ channel and the quadrupolar S channel satisfy the condition $(S+1/2)\omega_{\mathrm{rf}}^S + (I+1/2)\omega_{\mathrm{rf}}^I = \omega_r$. Actually there are many other CP conditions as long as the $(S+1/2)\omega_{\mathrm{rf}}^S \pm (I+1/2)\omega_{\mathrm{rf}}^I (I+1/2)\omega_{\mathrm{rf}}^L = n\omega_r$ ($n=1$ or 2) is satisfied.[50,51] However, we want to emphasize that an efficient CP requires not only the above specified condition but also the $(I+1/2)\times(\omega_{\mathrm{rf}}^{I_1} + \omega_{\mathrm{rf}}^{I_2}) \neq n\omega_r$ ($n=1$ or 2, $I = ^1H$ or ^{19}F) condition.

ACKNOWLEDGMENTS

This work was supported by the Director, Office of Science, Office of Basic Energy Sciences, Materials Sciences and Engineering Division, U. S. Department of Energy under Contract No. DE-AC03-76SF00098.

APPENDIX: FOURIER EXPANSION COEFFICIENTS OF THE SPINNING MODULATED SECOND-ORDER QUADRUPOLAR HAMILTONIAN

We give here the explicit expression for $\omega_Q^m(\alpha^Q,\beta^Q)$ required for the recoupling of the second-order quadrupolar interaction in the rotary resonance conditions as defined in Eq. (23):

$$\omega_Q^0=\frac{5}{96}A^2+\frac{1}{3}\left(\frac{B^2}{4}+\frac{C^2}{9}\right)+\frac{23}{48}\left(\frac{D^2}{4}+\frac{E^2}{9}\right), \tag{A1}$$

$$\omega_Q^{\pm 1}=\frac{1}{24\sqrt{2}}\left(\frac{BD}{4}-\frac{AB}{2}-\frac{CE}{9}\pm\frac{i}{6}(BE+CD-6AC)\right), \tag{A2}$$

$$\omega_Q^{\pm 2}=\frac{1}{48}\left(\frac{4C^2}{9}-AD-B^2\pm\frac{2i}{3}(2BC-AE)\right), \tag{A3}$$

$$\omega_Q^{\pm 3}=\frac{7}{24\sqrt{2}}\left(\frac{BD}{4}+\frac{CE}{9}\pm\frac{i}{6}(BE-CD)\right), \tag{A4}$$

$$\omega_Q^{\pm 4}=-\frac{7}{96}\left(\frac{D^2}{4}-\frac{E^2}{9}\pm\frac{i}{3}DE\right), \tag{A5}$$

where

$$A=3\cos^2\beta^Q-1+\eta_Q\sin^2\beta^Q\cos 2\alpha^Q, \tag{A6}$$

$$B=\sin^2\beta^Q\left(1-\frac{\eta_Q}{3}\cos 2\alpha^Q\right), \tag{A7}$$

$$C=\eta_Q\sin\beta^Q\sin 2\alpha^Q, \tag{A8}$$

$$D=\sin^2\beta^Q+\frac{\eta_Q}{3}(\cos^2\beta_Q+1)\cos 2\alpha^Q, \tag{A9}$$

$$E=\eta_Q\cos\beta^Q\sin 2\alpha^Q. \tag{A10}$$

[1] E. R. Andrew, A. Bradbury, and R. G. Eades, Nature (London) **183**, 1802 (1959).
[2] I. J. Lowe, Phys. Rev. Lett. **2**, 285 (1959).
[3] A. Pines, M. G. Gibby, and J. S. Waugh, J. Chem. Phys. **59**, 569 (1973).
[4] S. R. Hartmann and E. Hahn, Phys. Rev. **128**, 2042 (1962).
[5] U. Haeberlen, in *Advances in Magnetic Resonance*, edited by J. S. Waugh, Suppl. 1 (Academic, New York, 1976).
[6] J. Schaefer and E. O. Stejskal, J. Am. Chem. Soc. **98**, 1031 (1976).
[7] P. Tekely, P. Palmas, and D. Canet, J. Magn. Reson., Ser. A **107**, 129 (1994); A. E. Bennett, C. M. Rienstra, M. Auger, K. V. Lakshmi, and R. G. Griffin, J. Chem. Phys. **103**, 6951 (1995).
[8] M. Eden and M. H. Levitt, J. Chem. Phys. **111**, 1511 (1999).
[9] R. Tycko and G. Dabbagh, Chem. Phys. Lett. **173**, 461 (1990).
[10] T. Gullion and J. Schaefer, J. Magn. Reson. (1969-1992) **81**, 196 (1989).
[11] T. G. Oas, M. H. Levitt, and R. G. Griffin, J. Chem. Phys. **89**, 692 (1988).
[12] T. Gullion and S. Vega, Chem. Phys. Lett. **194**, 423 (1992).
[13] A. E. Bennett, J. H. Ok, R. G. Griffin, and S. Vega, J. Chem. Phys. **96**, 8624 (1992).
[14] N. C. Nielsen, H. Bildsoe, H. J. Jakobsen, and M. H. Levitt, J. Chem. Phys. **101**, 1805 (1994).
[15] Y. K. Lee, N. D. Kurur, M. Helmle, O. G. Johannessen, N. C. Nielsen, and M. H. Levitt, Chem. Phys. Lett. **242**, 304 (1995).
[16] S. Dusold and A. Sebald, Annu. Rep. NMR Spectrosc. **41**, 185 (2000).
[17] A. J. Vega, in *Encyclopedia of NMR*, edited by D. M. Grant and R. K. Harris (Wiley, New York, 1995), pp. 3869–3888.
[18] M. H. Cohen and F. Reif, Solid State Phys. **5**, 321 (1957).
[19] A. Abragam, *The Principles of Nuclear Magnetism* (Oxford University Press, Oxford, 1985).
[20] P. P. Man, in *Encyclopedia of NMR*, edited by D. M. Grant and R. K. Harris (Wiley, New York, 1995), p. 3838.
[21] A. J. Vega, J. Magn. Reson. (1969-1992) **96**, 50 (1992).
[22] C. P. Grey and W. S. Veeman, Chem. Phys. Lett. **192**, 379 (1992).
[23] C. P. Grey, W. S. Veeman, and A. J. Vega, J. Chem. Phys. **98**, 7711 (1993).
[24] C. P. Grey and A. J. Vega, J. Am. Chem. Soc. **117**, 8232 (1995).
[25] T. Gullion, Chem. Phys. Lett. **246**, 325 (1995).
[26] Y. Ba, H. M. Kao, C. P. Grey, L. Chopin, and T. Gullion, J. Magn. Reson. **133**, 104 (1998).
[27] L. Chopin, S. Vega, and T. Gullion, J. Am. Chem. Soc. **120**, 4406 (1998).
[28] M. J. Duer, Chem. Phys. Lett. **277**, 167 (1997).
[29] M. J. Duer and A. J. Painter, Chem. Phys. Lett. **313**, 763 (1999).
[30] N. G. Dowell, S. E. Ashbrook, J. McManus, and S. Wimperis, J. Am. Chem. Soc. **123**, 8135 (2001).
[31] L. Frydman and J. S. Harwood, J. Am. Chem. Soc. **117**, 5367 (1995).
[32] A. Medek, J. S. Harwood, and L. Frydman, J. Am. Chem. Soc. **117**, 12779 (1995).
[33] M. Edén and L. Frydman, J. Chem. Phys. **114**, 4116 (2001).
[34] G. Facey, T. P. Fong, D. Gusev, P. M. McDonald, R. H. Morris, M. Schlaf, and W. Xu, Can. J. Chem. **77**, 1899 (1999).
[35] G. Facey, D. Gusev, R. H. Morris, S. Macholl, and G. Buntkowsky, Phys. Chem. Chem. Phys. **2**, 935 (2000).
[36] K. Takegoshi, T. Yano, K. Takeda, and T. Terao, J. Am. Chem. Soc. **123**, 10786 (2001).
[37] S. Wi and L. Frydman, J. Am. Chem. Soc. **123**, 10354 (2001).
[38] T. Vosegaard, P. Florian, D. Massiot, and P. J. Grandinetti, J. Chem. Phys. **114**, 4618 (2001).
[39] J. D. Walls, K. H. Lim, and A. Pines, J. Chem. Phys. **116**, 79 (2002).
[40] M. Baldus, D. Rovnyak, and R. G. Griffin, J. Chem. Phys. **112**, 5902 (2000).
[41] S. Wi, H. Heise, and A. Pines, J. Am. Chem. Soc. (in press).
[42] E. Vinogradov, P. K. Madhu, and S. Vega, Chem. Phys. Lett. **329**, 207 (2000).
[43] S. Vega and A. Pines, J. Chem. Phys. **66**, 5624 (1977).
[44] K. Takegoshi, K. Nomura, and T. Terao, J. Magn. Reson. **127**, 206 (1997).
[45] S. Wi and L. Frydman, J. Chem. Phys. **112**, 3248 (2000).
[46] G. Engelhardt and H. Koller, Magn. Reson. Chem. **29**, 941 (1991).
[47] J. A. Lourens and R. Swanepoel, Solid State Commun. **7**, 1483 (1969).
[48] H. Nöth, Z. Naturforsch. B **39**, 1463 (1984).
[49] F. Taulelle, M. Pruski, J. P. Amoureux, D. Lang, A. Bailly, C. Huguenard, M. Haouas, C. Gerardin, T. Loiseau, and G. Ferey, J. Am. Chem. Soc. **121**, 12148 (1999).
[50] D. Rovnyak, M. Baldus, and R. G. Griffin, J. Magn. Reson. **142**, 145 (2000).
[51] J. P. Amoureux and M. Pruski, Mol. Phys. **100**, 1595 (2002).
[52] See EPAPS Document No. E-JCPSA6-007239 for the reintroduction of CSA. A direct link to this document may be found in the online article's HTML reference section. The document may also be reached via the EPAPS homepage (http://www.aip.org/pubservs/epaps.html) or from ftp.aip.org in the directory /epaps/. See the EPAPS homepage for more information.